

Cite this: DOI: 10.1039/c1sm05046j

www.rsc.org/softmatter

Photocontrol of end-grafted lambda-phage DNA

Yuting Liang Sun,^a Naresh Kumar Mani,^{bcd} Damien Baigl,^{bcd} Thomas Gisler,^e André Pierre Schröder^a and Carlos Manuel Marques^{*a}

Received 12th January 2011, Accepted 14th March 2011

DOI: 10.1039/c1sm05046j

We study the response to light stimulation of end-grafted λ -phage DNAs in a solution of AzoTAB, a photosensitive compacting agent of the DNA chains. The biotinilated double-stranded DNA molecules are end-attached to a streptavidinated substrate and incubated in a 120 mM tris-borate-EDTA buffer in the presence of the cationic surfactant AzoTAB. We find that the conformations and the dynamics of the tethered DNAs can be tuned by the AzoTAB concentration and strongly depend on illumination conditions. Under visible light or in the dark AzoTAB is in a *trans* configuration and it induces DNA adsorption onto the substrate for [AzoTAB] \geq 0.3 mM. In contrast, under UV illumination, AzoTAB is in a *cis* configuration and it induces DNA adsorption for [AzoTAB] \geq 0.4 mM. In the AzoTAB concentration range 0.3–0.4 mM, one can thus reversibly switch between the adsorbed and the non-adsorbed states of the end-grafted chains by exposing the sample respectively to visible light (>400 nm) and to UV illumination (365 nm). These light-induced adsorption transitions occur for AzoTAB concentrations approximately half of those required to control the DNA conformation in bulk solution, which highlights the predominance of chain-surface interactions over monomer-monomer intra-chain interactions for DNA molecules in the close vicinity of a solid substrate.

1 Introduction

Achieving light control of end-grafted chains has been the cornerstone in the design of photoresponsive systems such as microfluidic devices,¹ chemical gates and chemical valves,² nano-platforms for *in vivo* drug-delivery³ and many others where properties of surfaces are tuned by changes in the conformations of the attached polymer layers.⁴ Although extensive efforts have been made to correlate polymer architecture or conditions in the polymer environment to the final effects induced by the light, there is a lack of experimental geometries where the evolution of end-attached chain conformations can be directly monitored upon irradiation. Developments of such model experiments would not only pave the way for connecting individual chain conformations to global surface properties, but would also bring new insight into the long-standing problem of the collapsing and adsorption transitions in end-grafted polymers,^{5,6} as depicted in Fig. 1.

The conformations of single DNAs in bulk solution can be photocontrolled by adding to the DNA solution a cationic surfactant that contains a photosensitive moiety in its hydrophobic part.^{7,8} Several of these photosensitive surfactants have been successfully proposed, such as gemini surfactants⁹ and

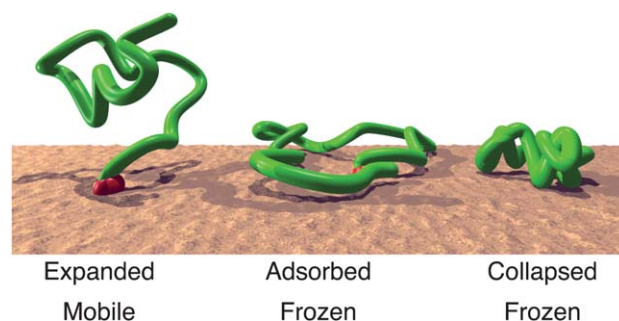


Fig. 1 A sketch of the three different conformations of end-grafted λ -phage DNA molecules observed in this study. In the left, at low AzoTAB concentrations, without enough attractive interactions between the chain and the substrate, the chain is fully mobile under thermal forces, with the restrictions imposed to the motion by the end-attached point and by the impenetrable wall. In the middle, at intermediate concentrations of AzoTAB, the presence of attractions between the chain and the substrate leads to adsorbed conformations that appear frozen at the optical length scales. In the right, a collapsed chain conformation at higher AzoTAB concentrations, when intra-chain attractions play a significant role.

^aInstitut Charles Sadron, Université de Strasbourg, CNRS UP 22, 23 rue du Loess, Strasbourg Cedex, 67083, France. E-mail: marques@unistra.fr; Fax: +33 388 414 099; Tel: +33 388 414 045

^bDepartment of Chemistry, Ecole Normale Supérieure, 75005 Paris, France

^cUniversité Pierre et Marie Curie Paris 6, 75005 Paris, France

^dUMR 8640, CNRS, France

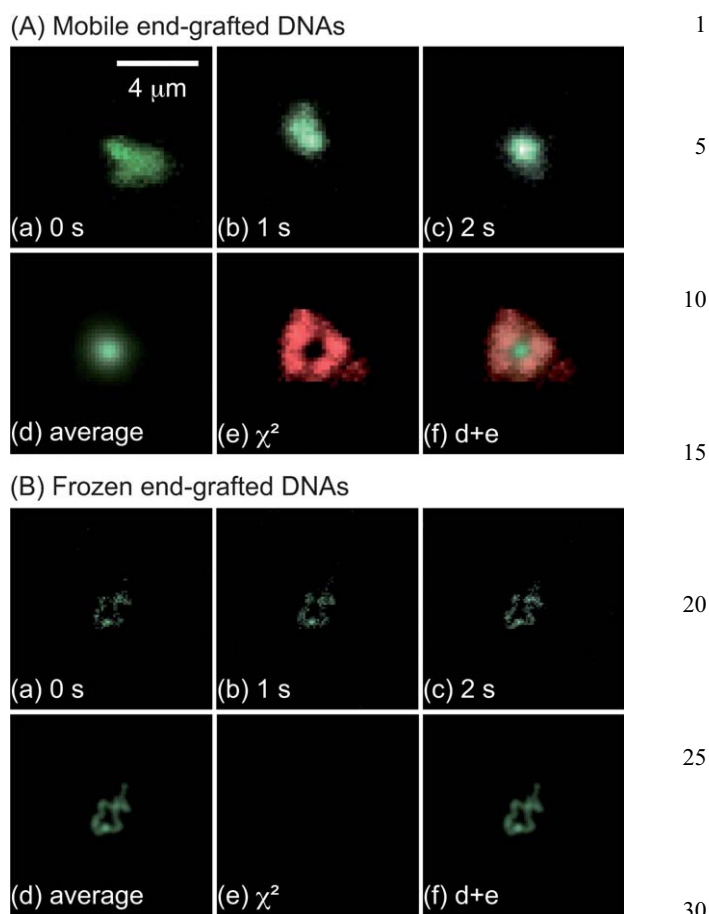
^eFachbereich Physik, Universität Konstanz, Fach M621, Konstanz, 78457, Germany

1 linear surfactants with various hydrophobicities,¹⁰ but the most
 2 widely used molecule is AzoTAB, a trimethylammonium
 3 bromide surfactant containing an azobenzene group in its short
 4 hydrophobic tail.^{7–11} When irradiated at 365 nm, AzoTAB
 5 undergoes a *trans* to *cis* isomerization accompanied by
 6 a change of polarity¹² (CMC = 12.6 mM and 14.6 mM for
 7 *trans* and *cis* isomers, respectively¹¹). It has been shown that
 8 this polarity change is accompanied by a change of its affinity
 9 for DNA.^{7–10} *Trans*-AzoTAB has a stronger affinity for DNA
 10 and induces DNA compaction at a lower concentration than its
 11 more polar form *cis*-AzoTAB. As a consequence there exists an
 12 AzoTAB concentration range for which DNA is compacted
 13 under visible light conditions (>400 nm) but unfolded under
 14 UV illumination (365 nm). These light-induced conformational
 15 changes have been studied in bulk^{7–10} and in cell-mimicking
 16 micro-environments⁸ and were applied to control gene expres-
 17 sion systems using light.¹¹

18 Unprecedented scrutiny of the equilibrium and out of equi-
 19 librium conformations of single DNAs near an impenetrable wall
 20 has been achieved by advances in the preparation of well defined
 21 surfaces with end-grafted DNA chains as well as by develop-
 22 ments in quantitative fluorescence microscopy of single-DNA
 23 molecules.^{13,14} In this paper we combine such techniques with
 24 the photocontrol power of AzoTAB to study for the first time the
 25 changes in conformations and dynamics of individual end-graf-
 26 ted DNA molecules in response to different light stimuli.

2 Results and discussion

27 The present study relies on our ability to determine the
 28 dynamic conformation state of end-grafted DNA chains in the
 29 presence of various concentrations of AzoTAB. In particular,
 30 we need to evaluate the progressive loss of mobility of the
 31 DNA chains as the AzoTAB concentration increases leading to
 32 a significant number of intra-chain and chain-substrate attrac-
 33 tive interactions. In previous work^{8,9} of free standing DNA
 34 chains in solutions, where only intra-chain bonds take place,
 35 the effect of attractive attractions induced by AzoTAB has
 36 been evaluated by studying the average optical size of DNA
 37 chains. In our case of end-grafted DNA chains, where chain-
 38 surface attractions play a significant role, chain size alone
 39 cannot discriminate between mobile and frozen states of the
 40 DNAs. We introduce here a new method—see Section 3.5—
 41 that enables assessing by simple image analysis the immobili-
 42 zation degree of an end-grafted DNA chain above optical
 43 image resolution, in our case for length scales above 0.3 μm .
 44 The results of this method are illustrated in Fig. 2 for DNA
 45 chains in 120 mM tris-borate-EDTA buffer (TBE) without—
 46 Fig. 2A(a–f)—and with—Fig. 2B(a–f)—added AzoTAB. When
 47 the chains are mobile, our method leads to a composite image
 48 in green and red—Fig. 2A(f)—where the green component
 49 indicates the average monomer concentration and the red
 50 channel shows our measure of mobility. Composite images only
 51 in green—Fig. 2B(f)—are observed for frozen DNAs, *i.e.* for
 52 chains that do not display any conformation changes at the
 53 optical length scales, within the few minutes available for
 54 experiments.

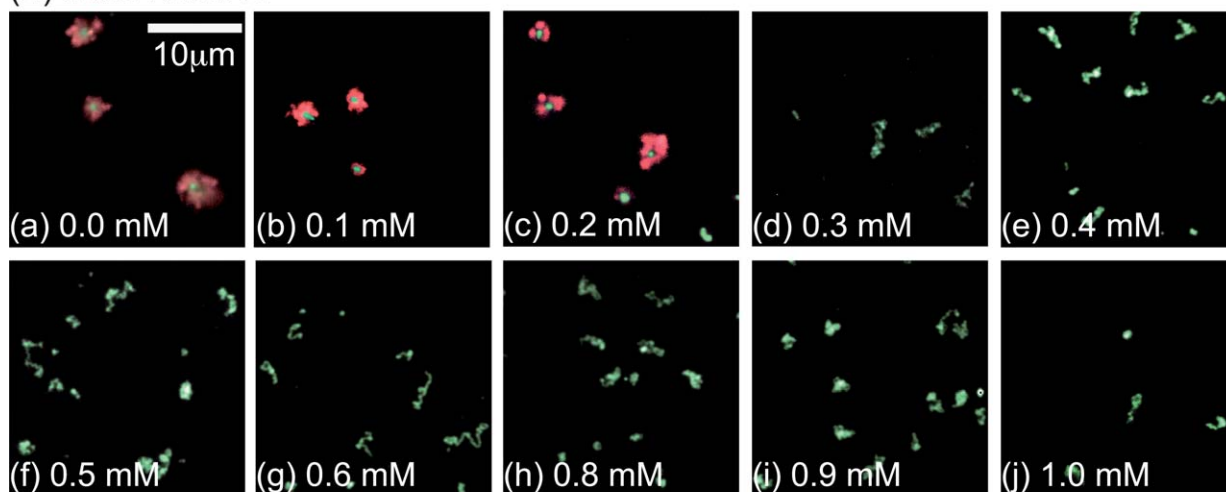


55 **Fig. 2** Assessment of DNA mobility by image analysis. (A) End-grafted
 56 DNA in 120 mM tris-borate-EDTA buffer (TBE). (a)–(c) Typical fluo-
 57 rescence microscopy snapshots: original fluorescence intensity was
 58 recorded with 16-bit resolution at 8 frames per second, and then dis-
 59 played in the green channel of a RGB image. (d) Average image of 37
 60 snapshots, where the fluctuations of conformation lead to an isotropic
 61 distribution of fluorescence intensity centered on the end-grafted posi-
 62 tion. (e) χ^2 -image—see text for a full description—displaying in the red
 63 channel the relative value of light intensity fluctuations for the 37 snap-
 64 shots. The center of the pattern is dark, and corresponds to a region with
 65 high light intensity and small relative fluctuations. Far from the center
 66 one recovers background fluctuations (noise of the camera) which have
 67 been subtracted. The larger values of χ^2 are thus exhibited at interme-
 68 diate distances from the center where DNA motion results in high relative
 69 light fluctuations. (f) Composite RGB image that combines the average (d)
 70 and χ^2 (e) images. According to the image analysis method developed
 71 here, single-DNA mobility and fluctuations of conformation result in
 72 the presence of a red halo in the composite images. (B) End-grafted DNA
 73 molecule in the same TBE buffer with added 0.6 mM of *trans*-AzoTAB.
 74 (a)–(f) Fluorescence snapshots, acquired, analyzed and displayed as in
 75 (A). Non isotropic distribution of light intensity in (d) and absence of red
 76 halo in (f) show that the DNA molecule is in a frozen conformation.

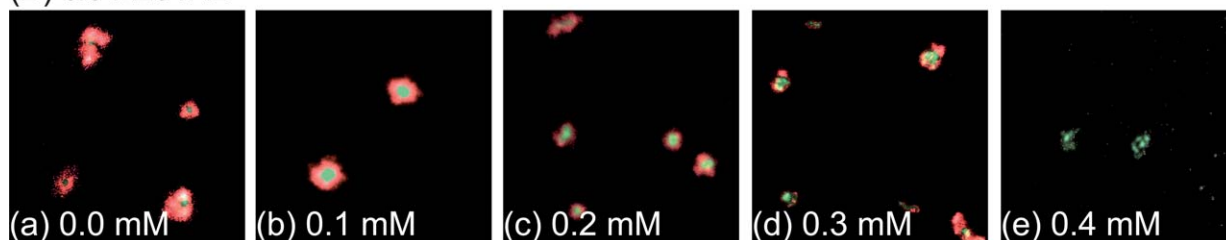
2.1 End-grafted DNAs in a *trans*-AzoTAB solution

77 We studied the end-grafted DNA conformations in a buffer
 78 (TBE) solution with increasing concentrations of *trans*-AzoTAB,
 79 in the range 0–2 mM. Fig. 3A shows typical composite images of
 80 DNA using the image analysis method described in Fig. 2. The
 81 images show that the chains exhibit significant mobility for
 82 AzoTAB concentrations below 0.3 mM. For concentrations

1 (A) *trans*-AzoTAB



20 (B) *cis*-AzoTAB



30 **Fig. 3** (A) Effect of the addition of different *trans*-AzoTAB concentrations to end-grafted DNAs in 120 mM tris-borate-EDTA buffer (TBE) solution. Red halos in figures (a)–(c) indicate DNA mobility as explained in Fig. 2. The chain conformations freeze for *trans*-AzoTAB concentrations above 0.3 mM. (B) A similar study with different *cis*-AzoTAB concentrations. With this AzoTAB isomer the chain conformations freeze only above 0.4 mM.

35 [AzoTAB] \geq 0.3 mM, the disappearance of the red halo indicates that all DNA molecules are in a frozen conformation. Images taken at 2 mM (not shown) also show a frozen configuration. We measured the fraction of the frozen chains for a given AzoTAB concentration by the fraction, computed over several composite images, of the green-only DNAs compared to the total DNA number. The results of the evolution of the frozen fraction with AzoTAB concentration are shown in Fig. 4. The figure also shows in the inset the compaction of T-4 DNA chains in the bulk, measured by their maximum extension under an optical microscope as described previously.⁸ T-4 DNAs are often used for such purposes since they are larger than λ -DNAs and allow for an easier and more precise size determination of the diffusing chains under a fluorescence microscope. Since the compaction in the bulk does not depend on chain size, this provides for a useful comparison with the corresponding behavior of end-grafted λ -DNA. As Fig. 4 shows, the freezing of the end-grafted chains occurs at concentrations below the nominal AzoTAB concentration required for complete chain collapse in the bulk, and the transition from a mobile to a frozen state is sharper than the coil to globule transition in the bulk. This shows that the surfactant binder is able to induce chain-surface interactions at concentrations where the known bulk-like intra-chain interactions start to play an effective role.

55 In order to further investigate this point, we measured the lateral extension of the end-grafted chains by computing the light-intensity weighted average of the square deviations $(x - x_{CM})^2$ and $(y - y_{CM})^2$ from the center of mass positions x_{CM} and

y_{CM} of the light distribution $I(x,y)$, $\langle (x - x_{CM})^2 + (y - y_{CM})^2 \rangle = \frac{\sum((x - x_{CM})^2 + (y - y_{CM})^2)I(x,y)}{\sum I(x,y)}$ with $x_{CM} = \frac{\sum x I(x,y)}{\sum I(x,y)}$ and $y_{CM} = \frac{\sum y I(x,y)}{\sum I(x,y)}$. The DNAs lateral extension $R = \langle (x - x_{CM})^2 + (y - y_{CM})^2 \rangle^{1/2}$ is displayed in Fig. 5. In the absence of AzoTAB, we obtained a value $R = 0.45 \mu\text{m} \pm 0.06 \mu\text{m}$, of the same order of magnitude of , the expected two-dimensional projection of the second moment of the monomer concentration distribution for a Gaussian chain of radius of gyration $R_g = (L^2 \nu_p / 3)^{1/2} \approx (16.5 \times 0.05 / 3)^{1/2} = 0.5 \mu\text{m}$, where we assume a DNA contour length $L \approx 16.5 \mu\text{m}$ and a persistence length $\nu_p \approx 0.05 \mu\text{m}$. As the AzoTAB concentration increases, the lateral size increases up to the freezing transition, where it stays roughly constant until it starts to decrease again for concentrations larger than 0.8 mM to reach a constant value above 1 mM.

Most DNA conformations at intermediate concentrations 0.3–0.8 mM can perhaps be better described as resulting from a random lacework. Under the optical microscope, the vertical position where the maximum fluorescence of such conformations can be captured is almost coincident with the surface itself, showing a much reduced vertical extension when compared to the free chains. Experimental evidence suggests then that the chains display an almost two-dimensional random walk, as sketched for the adsorbed chain in Fig. 1. However, a purely two-dimensional self-excluded random walk is not likely to have been achieved in our case. Indeed, by assuming that the polymer has $N = L/\nu_p \approx 330$ segments, one expects a relative increase of the lateral dimensions $R_{2D}/R \sim N^{3/4-\nu}$,¹⁵ with ν either the excluded

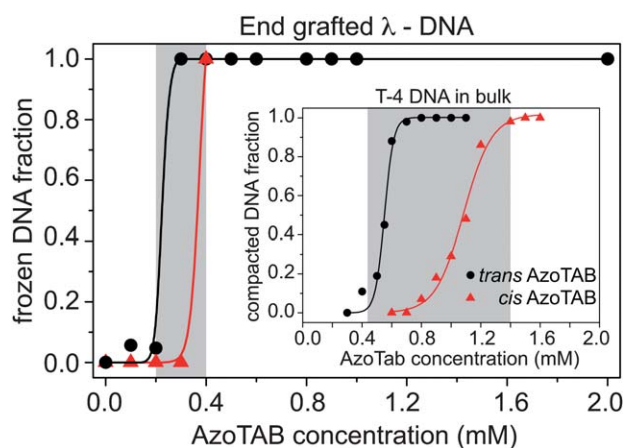


Fig. 4 Fraction of end-grafted lambda-phage DNAs with frozen conformations at different concentrations of (●) *trans* and (Δ) *cis*-AzoTAB, in TBE buffer solution. The immobilized fraction was counted from the number of DNAs without red halos in the composite images described in Fig. 2. While for *trans*-AzoTAB solutions the chain conformations freeze above 0.3 mM, a similar result is only achieved for *cis*-AzoTAB solutions above 0.4 mM. The grey region shows the concentration window where changes in DNA mobility can be expected upon isomerization of the AzoTAB molecule. The inset displays results from a study in bulk of T-4 DNA chains in the same buffer solution and different concentrations of (●) *trans* and (Δ) *cis*-AzoTAB. Compaction of the chains is achieved above 0.6 mM of *trans*-AzoTAB, and above 1.2 mM of its *cis* isomer. The grey area in the inset shows where the compaction state can be modified by a change of the isomeric form of AzoTAB. Note that this grey area in the bulk experiments is wider than the grey area for end-grafted chains. Also the compaction transition in the bulk is less sharp than the freezing transition on the surface.

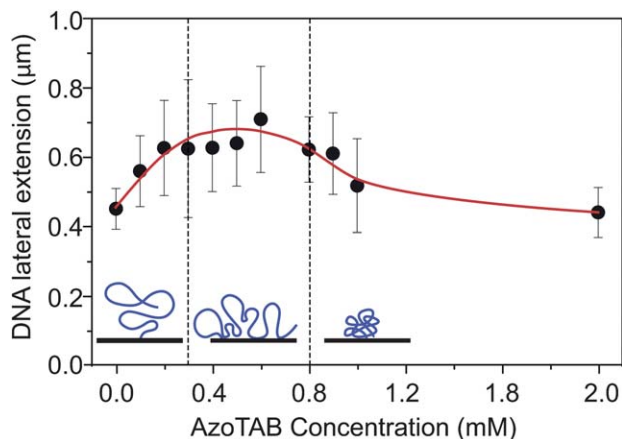


Fig. 5 Lateral extension of lambda-phage DNA's conformations in a TBE buffer with different concentrations of *trans*-azoTAB. Size is here measured by the square root of the mean square displacement in two-dimensions, computed from averages weighted by the light distribution. In the pure TBE buffer, the size of DNAs was $0.45 \mu\text{m} \pm 0.06 \mu\text{m}$. The first three points for which the average size increases correspond to mobile DNA conformations, while frozen conformations display roughly constant lateral dimensions. For concentrations above 0.8 mM the curve shows that the DNA size is noticeably reduced.

volume exponent $\nu = 0.6$ or, more likely, $\nu = 0.5$ for the case of semi-flexible chains as DNAs, where fully developed swelling statistics require much longer chains.^{16,17} Even a conservative estimate leads thus to $R_{2D}/R \sim 2.5$, significantly larger than the 1.5 value obtained in our experiments. Chains confined vertically over a distance D display instead a ratio $R_{2D}/R = (R/D)^{1/4}$. With $R_{2D}/R = 1.5$ we estimate the confinement distance at roughly $D \sim R/5 \sim 0.1 \mu\text{m}$, of the order of the smallest vertical displacement that we can detect with the z-positioning system of our microscope, and thus consistent with the observation that the maximum intensity is vertically coincident with the surface.

Images from chains in a solution with more than 0.8 mM AzoTAB present more compact conformations, also localized at the surface, that can be represented as the globule-like shape in Fig. 1. The transition above 0.8 mM from an extended adsorbed conformation to a compact adsorbed conformation is also compatible with data from bulk DNA—see inset of Fig. 4—showing that intra-chain attractions play a predominant role above such concentration, leading to the collapse of the chains. Note that under our experimental conditions, chains frozen first from solutions with intermediate AzoTAB concentrations 0.3–0.8 mM do not further compact following an increase in the concentration of the solution. This suggests that the observed compact conformations observed at the large concentrations are formed when intra-chain bonds can form before a strong attachment to the surface precludes further chain rearrangements.

2.2 End-grafted DNAs in a *cis*-AzoTAB solution

We also monitored the conformations of end-grafted λ -phage DNAs under the same conditions, except for the added AzoTAB isomer, used here in its *cis* configuration. This more polar form of the cationic surfactant¹² is known to exhibit a smaller affinity to the DNA molecules.¹⁰ In the bulk, for instance, the minimal concentration to achieve full compaction is 0.7 mM and 1.4 mM for *trans* and *cis* isomers, respectively (inset of Fig. 4). In the end-grafted configuration, the composite images of Fig. 3B show that the chains exhibit significant mobility up to 0.4 mM of *cis*-AzoTAB, to be compared to the threshold value of 0.3 mM for the *trans* isomer. Above 0.4 mM the chain behavior and the physical characteristics such as vertical or lateral dimensions are similar to those of the frozen conformations observed in *trans*-AzoTAB solutions. There is thus an AzoTAB concentration window between 0.3 mM and 0.4 mM where one might expect to induce a transition from a frozen to a free state of the DNA coils upon the isomerization of the molecule.

2.3 Effect of light on the adsorbed DNAs

Fig. 6(a) recalls that the conformations of end-grafted λ -DNAs freeze due to interactions with the surface, above a concentration of $[\textit{trans}\text{-AzoTAB}] > 0.3 \text{ mM}$, but require more than 0.4 mM for a solution of *cis*-AzoTAB. For an intermediate concentration, say of 0.35 mM of AzoTAB, one can induce transitions from the frozen, surface-adsorbed conformations to a mobile non-adsorbed state of the end-grafted chain by irradiating the sample with UV-light, thus inducing an isomeric transformation of the surfactant from its *trans* to its *cis* form. That partial or total

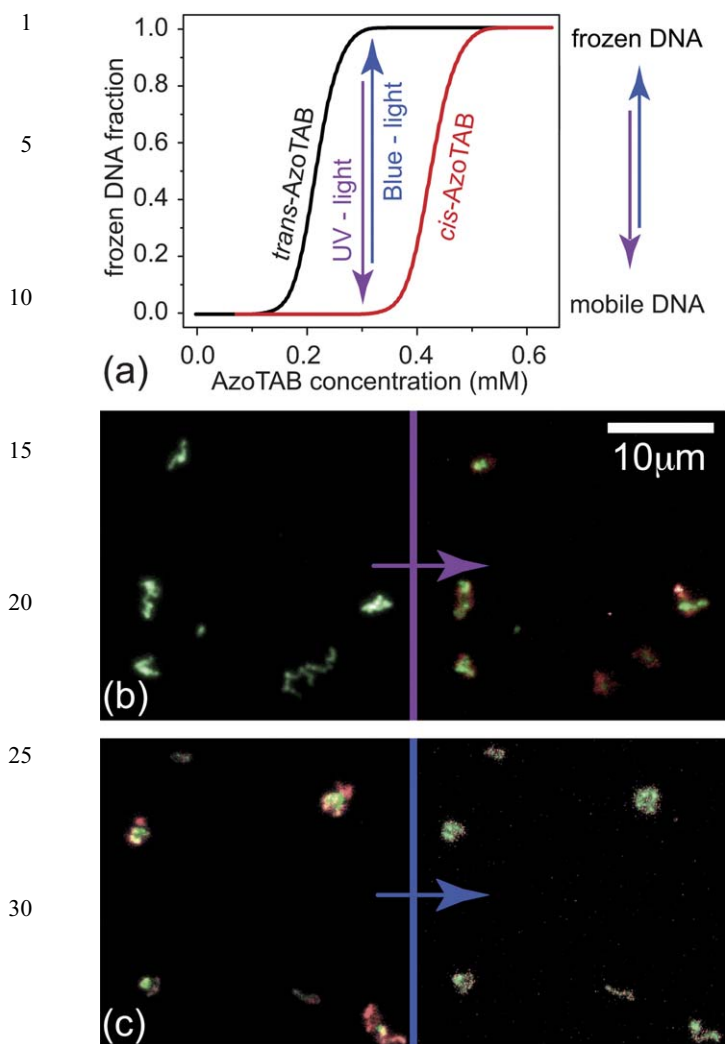


Fig. 6 Light induced changes in the conformations of end-grafted DNAs in 120 mM tris-borate-EDTA buffer (TBE) solution with 0.3 mM AzoTAB. (a) Scheme showing the AzoTAB concentration window where end-grafted lambda-DNAs can be photoswitched between a frozen and a mobile fluctuating state. (b) Initially frozen DNAs in a solution of 0.3 mM *trans*-AzoTAB recover their mobility after being exposed to UV irradiation (330–380 nm). (c) Initially mobile DNAs in a solution of 0.3 mM *cis*-AzoTAB freeze under blue light (450–490 nm).

mobility is recovered can be confirmed by direct observation under a microscope, and also by our mobility analysis displayed in Fig. 6(b). Conversely, illumination of the sample with blue light induces a transformation from the *cis* to the *trans* isomer, bringing initially mobile DNAs in a 0.35 mM *cis* solution into a frozen, adsorbed state as depicted in Fig. 6(c).

Finally, we investigate the kinetics of the light induced transformations. Fig. 7 shows a typical experiment performed by starting with a 0.3 mM *trans*-AzoTAB solution where chains are frozen. Exposure of the sample to UV irradiation under the microscope for 60 s leads to a transformation of the *trans* molecules in the field of view of the microscope into their *cis* isomer. After the UV light is turned off at time $t = 0$, the DNAs are observed under blue-light. They exhibit a significant mobility during the first few seconds but progressively freeze their conformations. This is due not only to the isomeric

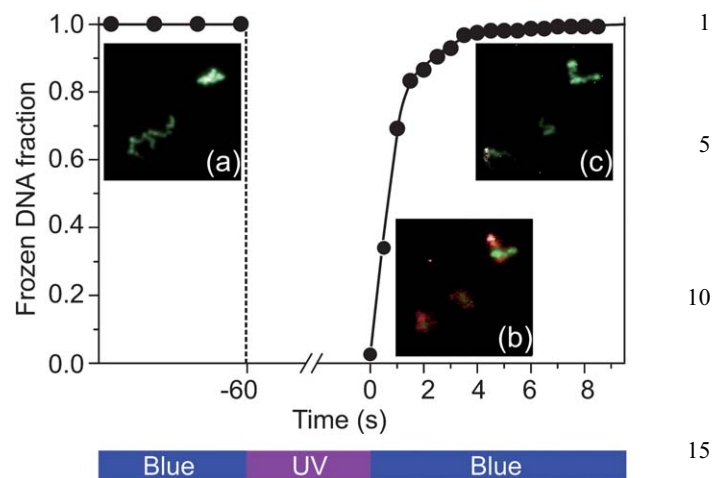


Fig. 7 Kinetics of the transformations between frozen and mobile states of end-grafted λ -phage DNAs in a TBE solution with 0.3 mM AzoTAB. The DNAs are initially frozen in 0.3 mM *trans*-AzoTAB. After being exposed for one minute to UV-illumination under the optical microscope, the DNAs recover their mobility. Diffusion into the observation field of neighboring *trans*-AzoTAB molecules gradually freezes again the DNAs conformations.

transformations under blue light but it is also due to the diffusion of *trans* molecules from the sample into the field of view. Indeed, molecules of a few nanometres in size have a diffusion coefficient of the order of $10^{-9} \text{ m}^2\text{s}^{-1}$, and take thus about 10 s to fully diffuse into a region of 10^{-8} m^2 , the typical area of the field of view under our operating conditions.

3 Materials and methods

3.1 Azotab synthesis

Azobenzene trimethylammonium bromide (AzoTAB) was synthesized as in Diguët *et al.*,¹² according to a procedure adapted from Hayashita *et al.*¹⁸ Surfactant purity was 99% determined by GC and by 250 MHz H and C NMR spectroscopy.

3.2 Functional DNAs, streptavidin-coated substrates and end-grafted DNA carpets

Double-stranded λ -phage DNAs (48502 base pairs, BioLabs) were end-functionalized with two single-stranded oligomers (MWG-Biotech): one end was labeled with biotin, while the other end was labeled with digoxigenin (DIG).¹⁴ After end-labelling, the DNAs were purified through a Nick column (Pharmacia Biotech), diluted in TBE (Tris-Borate-EDTA buffer, Sigma-Aldrich), and finally stained with YOYO-1 (Invitrogen), an intercalation fluorescent dye, at a 1 : 4 ratio of YOYO per base pair.

The method of preparation of single end-grafted DNA carpets has been described previously by Hissette *et al.*¹⁴ Briefly, cover glasses of 30 mm, from Menzel-Glaser were first cleaned with a piranha solution (75% of H_2SO_4 (97% Sigma-Aldrich) and 25% of H_2O_2 (30%, Sigma-Aldrich)), and then immediately used after rinsing with milli-Q water. The cleaned glasses were immersed

1 into an ethanol solution of 2% APTES (3-amino-
propyltriethoxysilane, Sigma-Aldrich) for 1 h, then rinsed first
with ethanol and then with milli-Q water. The silane layer is
5 stabilized in the oven at 100 °C for one hour and finally kept in
dark dry conditions until further use. These silanised glasses were
then incubated with glutaraldehyde (8%, Polysciences) for 30
min, rinsed with PBS, and then incubated with a PBS solution of
0.1 mg mL⁻¹ streptavidin (Sigma-Aldrich) for one hour. After
10 a final rinsing in TBE, the streptavidinated substrates were kept
under humid conditions and used within 2 h.

Streptavidinated substrates were incubated for a few minutes
with a 2 µg mL⁻¹ biotinylated DNA solution, and gently rinsed
with TBE. Special care was taken to avoid any contact between
the DNA carpet and air. Due to the strong specific adhesion
15 between biotin and streptavidin, the procedure led to dilute
single end-grafted DNA carpets as readily observed by optical
fluorescence microscopy.

3.3 Fluorescence microscopy

20 Fluorescence images were obtained using indifferently inverted
microscopes TE200 or TE2000 (Nikon, Japan), equipped with
a 100× oil immersion objective. A fluorescence filter block (EX
450–490/DM 505/BA 520 nm) was used for DNA observation,
and a second block (EX 330–380/DM 400/BA 420 nm) was used
25 to induce the *cis* to *trans* conformation transition of AzoTAB.
Pictures were recorded *via* a digital camera (Hamamatsu EM-
CCD, Japan) at a rate of *circa* 10 frames per second, and
analyzed using homemade software.

3.4 Observation cell

A homemade observation cell was used to observe the end
grafted DNA carpets. The cell enables the slow exchange of the
liquid surrounding the carpet directly under the microscope.
Briefly, a Teflon® spacer is placed in between two glass slides,
one of which being the cover glass supporting the DNA carpet.
Two Teflon® tubes (diameter 1.0 mm) are inserted into the
spacer. One of the tubes is connected to a syringe while the other
is connected to a container. Injection of one millilitre of a liquid
40 into the cell results in a complete exchange of the liquid
contained in the cell. Special care has been taken to avoid too strong
shear rates during the liquid exchange stage, by ensuring, under
45 the microscope, that the DNAs were almost unperturbed by the
induced fluid flow.

3.5 Motion detection from image analysis

Our motion analysis is performed on a sequence of several tens of
images of a given region of the surface with end-grafted DNAs,
50 captured at a typical rate of five images per second, *i.e.* corre-
sponding to roughly ten second sequences. Our observation was
performed under attenuated light for the YOYO excitation, thus
reducing photo-bleaching, and a high gain level compensating
for the relatively low emission power of YOYO, with a good
55 background to signal ratio: this was obtained with an EM-CCD
camera (Hamamatsu, Japan). The time dependence of the
intensity for each pixel of the image is first stored over the whole
time sequence, then, a linear fit of these data is calculated for each
pixel, with the corresponding average square difference between

the data and the fitting line a quantity known as χ^2 . Finally,
1 a new image is built that converts the χ^2 values of each pixel to
a grey-level image that can be visualized on the screen, by simply
renormalizing the range of measured χ^2 values over the whole
5 image, to the 0–65535 range of a 16 bit image. Such a measure-
ment is shown in Fig. 2A(e) in the red channel of a RGB image.
As the figure shows, the pixels of the image in the center of the
DNA region appear as dark pixels, corresponding to weak values
of χ^2 . Here in the center, above the grafting point, the signal is
10 dominated by consistently high values of the average light
intensity and therefore by low relative fluctuations around the
average. Conversely, the immediate periphery of the central dark
region displays a ring-like region of higher χ^2 values. In this
region, the intensity fluctuations are comparable to, or larger
15 than, the average intensity. Far from the DNA the image is dark,
showing a good signal-to-noise ratio. By superimposing this
image with Fig. 2A(d) that represents the fluorescence average
intensity image of the same region displayed in the green RGB
channel, one obtains the composite Fig. 2A(f). The red halo of
20 the composite image allows easy identification of the fact that the
chains exhibited a significant mobility in the image sequence
analyzed. When the DNA mobility is reduced either by strong
attractive interactions with the surface, or by intra-chain
attractions, the red halo vanishes, as displayed in Fig. 2B(e,f). In
25 general, one would expect these halos to be circularly symmetric,
which is indeed the case when the measurement is made over
a large enough number of images.

4 Conclusions

30 Exposure of DNA molecules to a solution of nucleic acid binders
is known to result in collapse of the chains above a typical
threshold concentration, due to intra-chain attractive interac-
tions mediated by the binders. Concentration thresholds are
a function of the affinity of the binders, high affinity binders
35 inducing DNA condensation at lower concentrations. The
cationic surfactant AzoTAB⁸ used in this work is a DNA binder
with two photoresponsive isomeric states. Illumination of the
molecule with UV-light leads to the *cis* form of the isomer that
has lesser affinity than the *trans* isomer. Transition from the *cis* to
40 the *trans* isomers can be obtained for instance by irradiation with
blue light. The different binding affinities of the isomers result in
two different condensation thresholds, found for instance for T-4
DNAs in a 120 mM tris-borate-EDTA buffer (TBE) solution at
45 0.6 mM and 1.2 mM AzoTAB. Within this concentration
window, collapse and expansion of the DNAs can be obtained by
photo-switching between the two isomeric forms.

In our work, we studied λ -phage DNAs end-grafted to
a streptavidinated surface and found attractive interactions
between the DNAs and the streptavidin substrate, occurring at
50 lower binder concentrations than the corresponding bulk
thresholds, at 0.3 mM and 0.4 mM AzoTAB, respectively, for the
trans and the *cis* forms. The hierarchy of affinities between the
two isomers is thus the same as the corresponding hierarchy in
the bulk. We characterized the end-grafted chain fluctuations
55 observed by fluorescence microscopy with a new method that is
able to assign a mobility measure to each image pixel, and
therefore to color code for a straightforward interpretation of the
fluorescence images.

1 The induced attractions result in a transition, that we quantified with our method, from mobile, fluctuating DNAs to DNAs with frozen conformations. Here binding between the monomers and the surface results in a flattening of the chain and in the absence of fluctuations of the chain segments at the optical level. Strikingly, these chain adsorption transitions are sharper than the corresponding bulk condensations, and the threshold window where photo-switching can be achieved is narrower. In this window, we showed that initially mobile end-grafted chains can be photo-driven into adsorption by blue light, and that initially frozen DNAs can be freed by exposure to UV irradiation in the field of view of the microscope. In this last case, return to a frozen state when the UV light is turned off occurs in a few seconds, compatible with fast chain-surface binding, limited only by the diffusion of the binders into intimate contact with the end-grafted chains.

Our work raises not only a number of important questions but also paves the way for further developments of photoresponsive interfacial polymer structures. For instance, our DNA carpets offer new exciting possibilities for performing photocontrolled transcription/expression experiments¹¹ on individual, substrate born DNAs. The induced attractions with the surface have precluded in our configuration the fundamental study of the influence of end-grafting on the collapsing transition of long DNA chains. Such a study is within a reasonable reach, requiring further protection of the surfaces against chain binding. Our time sensitivity was also restricted to a few images per second, and only diffusion limited phenomena over a few seconds could be studied in detail. Pushing the limits of time detection would certainly bring in crucial new information about the first moments of the chain-surface binding kinetics.

Acknowledgements

This work was supported by the French Ministry for Higher Education through the German-French IRTG on the Physics of

Soft Condensed Matter. Inspirational input from T. Schmatko is also acknowledged.

References

- 1 B. Zhao, J. S. Moore and D. J. Beebe, *Science*, 2001, **291**, 1023–6.
- 2 Y. Park, Y. Ito and Y. Imanishi, *Macromolecules*, 1998, **31**, 2606–2610.
- 3 D. A. LaVan, T. McGuire and R. Langer, *Nat. Biotechnol.*, 2003, **21**, 1184–91.
- 4 S. Samanta and J. Locklin, *Langmuir*, 2008, **24**, 9558–65.
- 5 E. Eisenriegler, *Polymers near surfaces: conformation properties and relation to critical phenomena*, World Scientific, Singapore, 1993.
- 6 S. Metzger, M. Müller, K. Binder and J. Baschnagel, *J. Chem. Phys.*, 2002, **11**, 985–995.
- 7 A. L. M. Le Ny and C. T. Lee, *J. Am. Chem. Soc.*, 2006, **128**, 6400–6408.
- 8 M. Sollogoub, S. Guieu, M. Geoffroy, A. Yamada, A. Estevez-Torres, K. Yoshikawa and D. Baigl, *ChemBioChem*, 2008, **9**, 1201–1206.
- 9 M. Geoffroy, D. Faure, R. Oda, D. M. Bassani and D. Baigl, *ChemBioChem*, 2008, **9**, 2382–2385.
- 10 A. Diguët, N. K. Mani, M. Geoffroy, M. Sollogoub and D. Baigl, *Chem.–Eur. J.*, 2010, **16**, 11890–6.
- 11 A. Estevez-Torres, C. Crozatier, A. Diguët, T. Hara, H. Saito, K. Yoshikawa and D. Baigl, *Proc. Natl. Acad. Sci. U. S. A.*, 2009, **106**, 12219–12223.
- 12 A. Diguët, R.-M. Guillemic, N. Magome, A. Saint-Jalmes, Y. Chen, K. Yoshikawa and D. Baigl, *Angew. Chem., Int. Ed.*, 2009, **48**, 9281–4.
- 13 J. T. Mannion, C. H. Reccius, J. D. Cross and H. G. Craighead, *Biophys. J.*, 2006, **90**, 4538–45.
- 14 M. L. Hisette, P. Haddad, T. Gisler, C. M. Marques and A. P. Schroder, *Soft Matter*, 2008, **4**, 828–832.
- 15 P. G. de Gennes, *Scaling concepts in polymer physics*, Cornell University Press, Ithaca, N.Y., 1979.
- 16 D. Schaefer, J. Joanny and P. Pincus, *Macromolecules*, 1980, **13**, 1280–1289.
- 17 F. Thalmann, V. Billot and C. M. Marques, *Physical Review E*, 2010, submitted.
- 18 T. Hayashita, T. Kurosawa, T. Miyata, K. Tanaka and M. Igawa, *Colloid Polym. Sci.*, 1994, **272**, 1611–1619.

1 Authors Queries 1

Journal: SM

5 Paper: c1sm05046j 5

Title: Photocontrol of end-grafted lambda-phage DNA

Editor's queries are marked like this... **1**, and for your convenience line numbers are inserted like this... 5

Query Reference	Query	Remarks
15 1	For your information: You can cite this paper before the page numbers are assigned with: (authors), Soft Matter, (year), DOI: 10.1039/c1sm05046j.	
20 2	The sentence beginning "Special cares has been taken to avoid..." has been altered for clarity. Please check the intended meaning has not changed.	
25 3	Ref. 17: Can this reference be updated yet? Please supply details to allow readers to access the reference (for references where page numbers are not yet known, please supply the DOI).	